



HAL
open science

Potential of field hyperspectral imaging as a non destructive method to assess leaf nitrogen content in Wheat

Nicolas Vigneau, M. Ecarnot, Gilles Rabatel, P. Roumet

► **To cite this version:**

Nicolas Vigneau, M. Ecarnot, Gilles Rabatel, P. Roumet. Potential of field hyperspectral imaging as a non destructive method to assess leaf nitrogen content in Wheat. *Field Crops Research*, 2011, 122 (1), p. 25 - p. 31. 10.1016/j.fcr.2011.02.003 . hal-00613201

HAL Id: hal-00613201

<https://hal.science/hal-00613201>

Submitted on 3 Aug 2011

HAL is a multi-disciplinary open access archive for the deposit and dissemination of scientific research documents, whether they are published or not. The documents may come from teaching and research institutions in France or abroad, or from public or private research centers.

L'archive ouverte pluridisciplinaire **HAL**, est destinée au dépôt et à la diffusion de documents scientifiques de niveau recherche, publiés ou non, émanant des établissements d'enseignement et de recherche français ou étrangers, des laboratoires publics ou privés.

Potential of field hyperspectral imaging as a non destructive method to assess leaf nitrogen content in Wheat

Nathalie Vigneau^a, Martin Ecartot^b, Gilles Rabatel^a, Pierre Roumet^{b,*},

^a*Cemagref, UMR ITAP, 361 rue Jean-François Breton, F-34196 Montpellier, France.*

^b*INRA, UMR DIA-PC, Domaine de Melgueil, F-34130 Mauguio, France.*

Abstract

Nitrogen is the most important crop limiting factor, thus plant nitrogen status during plant cycle is a key parameter for crop monitoring. Many new techniques, based on leaf optical properties have been proposed for a non-destructive diagnosis to replace Nitrogen Nutrition Index which is a costly and destructive method. We intend here to study leaf nitrogen concentration accessibility from reflectance (400-1000 nm) spectra of whole plants from a field hyperspectral imaging set-up including difficulties related to variable solar lighting and potential specular reflexion. Firstly, we calibrated a chemometrical model between leaf nitrogen concentration and reflectance spectra of flat leaves ($R^2=0.903$, SEP=0.327 %DM), which validated the sensor and our reflectance correction process. As a second step, we calibrated a chemometrical model between nitrogen concentration and reflectance spectra of individual leaves from isolated plants grown in pots in greenhouse ($R^2=0.889$, SEP=0.481 %DM) or under field conditions ($R^2=0.881$, SEP=0.366 %DM).

*Corresponding author

Email address: roumet@supagro.inra.fr (Pierre Roumet)

Pooling the two datasets provided us a relevant model to predict leaf nitrogen content for the two culture conditions ($R^2=0.875$, $SEP=0.496$ %DM) suggesting that this technique is promising to assess nitrogen plant parameters with a non destructive method. This tool could be used to follow-up plant nitrogen dynamics criteria or to generate nitrogen spatial cartographies.

Keywords: hyperspectral, reflectance, nitrogen concentration, durum wheat

1 **1. Introduction**

2 As nitrogen availability in soil affects both yield and harvest quality in
3 most annual cultivated species, nitrogen (N) is considered as key plant nutri-
4 ment. During vegetative growth soil N is taken up by roots and assimilated
5 in leaves to synthesize proteins, which are integrated in structural compo-
6 nents to constitute cell wall or enzymes in metabolic pathways. In leaves,
7 main part of nitrogen is involved in photosynthetic process through the Ru-
8 bisco (which represents about 50 % of leaf nitrogen content, Evans (1983))
9 or enzymes implied in transportation or assimilation of fixed carbon.

10

11 As soil N supply is often limited, nitrogen fertilizer management should
12 be adjusted to crop N requirements to optimize plant production (Lemaire
13 et al., 2008). To evaluate this plant demand, a well established diagnostic
14 tool is the Nitrogen Nutrition Index(NNI) (Lemaire and Gastal, 1997). NNI
15 is based on comparing actual crop bulk N concentration with an empirical N
16 dilution curve. The biomass dependent, critical N concentration (N_c) is the
17 minimal N concentration required for maximal growth, developed by Lemaire

18 and Salette (1984) and then adapted for most cultivated plants (Justes et al.
19 (1994) for winter wheat, Sheehy et al. (1998) for rice, Colnenne et al. (1998)
20 for rape, Bélanger et al. (2001) for potato and Ziadi et al. (2010) for spring
21 wheat). Obviously the method is laborious and destructive. In other hand, as
22 a strong relationship exists between leaf nitrogen content and photosynthetic
23 pathway, N leaf indirect estimations based on chlorophyll measurement have
24 been suggested (Baret and Fourty, 1997). Indirect and non destructive N
25 methods derived from chlorophyll measurement through leaf transmittance
26 were proposed; such as Chlorophyll meter SPAD 502®[®], which provides leaf
27 chlorophyll content based on leaf transmittance at two wavelengths : 650
28 and 940 nm.

29

30 If some authors, as Lee et al. (1999) found a good relationship (R^2 between
31 0.81 and 0.96 according to the stages of growth) between the chlorophyll
32 content and the actual nitrogen concentration (%DM), others works demon-
33 strated that this linear relationship nitrogen/chlorophyll does not work in
34 every condition; it could vary according to environmental conditions or/and
35 cultivars (Spaner et al., 2005). To stabilize this relationship the use of ratio
36 between data from experimental plots with overfertilizer reference plot have
37 been recommended (Ziadi et al., 2008) although this reference plot may be
38 sometimes difficult to put in place as underlined by Fox et al. (2001). Any-
39 way, Houlès et al. (2007) connect successfully chlorophyll and NNI with a
40 linear equation (R^2 between 0.63 and 0.71 according to growing stage) and
41 Ziadi et al. (2008) measured a determination coefficient of 0.61 between NNI
42 and SPAD values. An integrated approach consists in calculating the NNI

43 using remote sensing: the biomass is found through the LAI and the nitrogen
44 content through the chlorophyll content at the canopy scale (Houlès et al.,
45 2007; Lemaire et al., 2008; Chen et al., 2010; Fitzgerald et al., 2010).

46

47 In these approaches, the chlorophyll-nitrogen relationship quality is the
48 key point of the nitrogen prediction quality. Yet, this chlorophyll-nitrogen
49 relationship depends on growing season (Evans, 1983) or on nitrogen content
50 range as shown by Evans (1983) and Hidema et al. (1991) at leaf level.

51

52 An alternative approach was proposed by Kokaly (2001); it consists to
53 estimate directly plant nitrogen content from a greater wavelength number
54 from visible and infrared spectra as it was classically done in spectroscopy.
55 Wavelength range characteristics and chemometrical models have been in-
56 vestigated to carry out the more efficient models to predict N plant concen-
57 tration.

58

59 Hansen and Schjoerring (2003) demonstrated that visible and NIR spec-
60 tra from 400 to 900 nm coupled with a Partial least Square regression (PLS)
61 allows to calibrate N plant content with R^2 of 0.71 and an error of prediction
62 of 0.38 % of dry matter, improving of 24 % nitrogen concentration prediction
63 based on vegetation indices as the NDVI for example. Similar results were
64 reported by Alchanatis and Schmilovitch (2005) from spectra of leaves in the
65 field measured from 530 to 1100 nm ($R^2 = 0.81$ and an error of prediction
66 of 0.27 %DM) and by Morón et al. (2007) with spectra (400-2500 nm) col-
67 lected spectra from excised fresh material ($R^2 = 0.89$, with prediction errors

68 of 0.64). In this later work, authors pointed out that a robust model could
69 be obtained on fresh material, if appropriate sampling data set representing
70 a large range of environmental conditions and different cultivars was used.

71

72 These results suggested that an alternative approach based on an ex-
73 tended number of wavelength coupled with chemometrics could provide direct
74 estimation of nitrogen leaf content. By diversifying calibration samples (cul-
75 ture conditions, genotypes, etc.), the variability of the relation chlorophyll-
76 nitrogen should be included in the model.

77 For this purpose, we built a close-range hyperspectral imaging set-up to take
78 images above wheat plots. In this context, hyperspectral imagery combines
79 several advantages: first, it brings a sufficient spectral resolution for a direct
80 access to nitrogen content, as discussed above. Second, its spatial resolution
81 allows collecting the spectra of individual leaves when observing a whole plot.
82 Since nitrogen content of the well illuminated leaves at the top of the canopy
83 is well correlated to the crop NNI (Farrugia, 2004), the measurement of their
84 individual spectra enables to access NNI in a non-destructive way. Moreover,
85 spatial nitrogen distribution makes it possible to analyse individual plants
86 within crops; this provides an innovative tool to quantify heterogeneity in-
87 side canopy, in context of monogenetic cultivars as well as multigenotypic or
88 multispecific crops.

89

90 The hyperspectral imagery also presents several advantages compared
91 with punctual spectrometers (such as SPAD 502®). First, it gives spectra
92 of each visible leaf of the plot in one image, which is considerably time

93 saving. Furthermore, these spectra are available for each pixel of the leaf
94 surface, providing a better representativeness of the leaf spectral information,
95 compared to a single spectrometric measurement.

96 In counterpart, such a close-range imaging system presents some specific
97 difficulties related to the management of variable solar lighting, specular
98 reflection and variable illumination level due to leaf inclination. In this pa-
99 per, we describe successive correction procedures to obtain light-independent
100 reflectance spectra from the original images. Then the calibration of chemo-
101 metrics models between N content and reflectance spectra for isolated wheat
102 plants in various conditions (field and greenhouse) are presented and dis-
103 cussed.

104 **2. Material and methods**

105 *2.1. Hyperspectral image acquisition system*

106 All hyperspectral images were acquired with a pushbroom CCD camera
107 (HySpex VNIR 1600-160, Norsk Elektro Optikk, Norway) fitted on a tractor-
108 mounted motorised rail (see Figure 1). The camera spectral range was from
109 400 nm to 1000 nm divided in 160 bands (3.7 nm spectral resolution). The
110 first image spatial dimension was determined by the 1600 across-track pixels
111 of the CCD matrix and the second one came from the camera forward move-
112 ment on the ramp. At 1 m above the vegetation and with a nadir sighting,
113 the ground track was about 30 cm and the spatial resolution across track
114 was 0.2 mm (the lens and the view angle are fixed). The spatial resolution
115 along track was set to 0.5 mm. The integration time, i.e. the time duration
116 during which sensor is storing light energy, was fixed manually by the user

117 depending on meteorological conditions (cloudy or sunny weather). Images
118 were then corrected in radiance using sensor characteristics (e.g. spectral
119 sensitivity, etc.) provided by the manufacturer.

120

121 *2.2. Reflectance correction*

122 As a first approximation (i.e. if we consider Lambertian surfaces), radi-
123 ance $L(\lambda)$ is the product of the target reflectance $R(\lambda)$, which is intrinsic
124 information and the illumination during image acquisition, i.e. in our case
125 solar lighting $E(\lambda)$.

126

$$L(\lambda) = R(\lambda) \cdot E(\lambda) \quad (1)$$

127 Radiance can not be used directly because illumination depends on date
128 and meteorological conditions. To obtain the variable of interest R , it is
129 thus necessary to know the illumination. For that purpose, spectralon®
130 (Labsphere, Inc., New Hampshire, USA) placed in the field of view of the
131 sensor is commonly used because it is a perfect Lambertian diffuser. Another
132 alternative is to use a reference whose spectral characteristics are known.
133 Indeed, in given lighting conditions:

$$L_{target} = R_{target} \cdot E \quad (2)$$

$$L_{ref} = R_{ref} \cdot E \quad (3)$$

$$R_{target} = \frac{L_{target}}{L_{ref}} \cdot R_{ref} \quad (4)$$

134 where R designs the reflectance, L the radiance, and ref the reference.
135 In this study, we used a ceramic plate appropriate for an every day field use.
136 R_{ref} was obtained from laboratory measurements.

137 An example of raw, radiance and reflectance spectra is presented in Figure
138 2.

139 Only reflectance spectra are used for model calibration.

140

141 This process is theoretically correct for flat leaves but not for inclined
142 leaves. Indeed, the leaf inclination toward the sun implies two phenomena
143 which must be taken into account. Due to their dissimilar orientation toward
144 the sun, all leaves do not receive the same level of illumination. They do not
145 receive either the same level than the reference ceramic. Each illumination
146 level is linked to the cosine of the angle between the surface and the light
147 incidence. Because this difference is independent of the wavelength, it can
148 be introduced as a multiplicative factor. So $E_{leaf}(\lambda) = k_1 E_{ref}(\lambda)$ with E_{leaf}
149 is the lighting received by an inclined leaf and E_{ref} , the lighting received
150 by the horizontal ceramic plate.

151

152 Moreover, the Lambertian approximation above is not exact. Leaves can
153 undergo specular reflexion, i.e. a fraction k of the incident light is reflected by
154 the leaf with no spectral modification (Grant, 1987; Bousquet et al., 2005;
155 Chelle, 2006). Because this specular reflexion is independent of the wave-
156 length (Bousquet et al., 2005), we can write:

$$R_{leaf}(\lambda) = \rho(\lambda) + k \quad (5)$$

$$L_{leaf} = (\rho(\lambda) + k) \cdot k_1 E_{ref} \quad (6)$$

157 where $\rho(\lambda)$ is the Lambertian part of the leaf reflectance and k is the
158 specular part.

Therefore applying the correction process (equation 4) leads to :

$$\frac{L_{leaf}}{L_{ref}} \cdot R_{ref} = \frac{(\rho(\lambda) + k) \cdot k_1 E}{E}$$
$$R_{app} = k_1 \cdot \rho(\lambda) + k_2 \quad (7)$$

159 where R_{app} is the reflectance obtained after the correction process, $\rho(\lambda)$
160 is the Lambertian part of the leaf reflectance and k_1 and k_2 are two scalar
161 factors independent of the wavelength.

162

163 As a summary, the solar lighting and the leaf inclination imply a multi-
164 plicative effect and an additive effect on the obtained reflectance with our
165 correction process.

166 2.3. Chemometrical model calibration

167 We calibrated chemometrical models between reflectance spectra (400-
168 1000 nm) and nitrogen concentration values of individual leaves using Par-
169 tial Least Square regression (PLS) (Martens and Næs, 1998; Wold et al.,
170 2001). Each dataset, if the number allowed it, was split in a calibration set

171 (2/3 of the samples) and a test set (the last third) with the same distribu-
172 tion of nitrogen concentration. We calibrated the model by cross-validation
173 leave-one-out on the calibration set. The best calibration equation and the
174 number of latent variables (LV) were selected on the basis of a large coefficient
175 of multiple determination (R^2) and a low standard error of cross-validation
176 (SECV). SECV is the root mean square error between the actual and pre-
177 dicted values calculated over all cross-validation calibrations. The model was
178 then tested on the test set and its quality was evaluated with the standard
179 error of prediction corrected of the bias (SEP_c) calculated as following:

$$SEP_c = \sqrt{\frac{\sum(\hat{y}_i - y_i - bias)^2}{N}} \quad (8)$$

180 where N is the number of sampling of test set, y_i , the actual value of the
181 sampling i and \hat{y}_i the predicted value for the sampling i . The bias is the
182 mean value of the difference between actual and predicted values (this value
183 can thus be negative). It represents the distance between the prediction and
184 the first bisector. In the following, we will present for each model the SEP_c
185 and the bias separately.

186

187 In order to overcome leaf inclination and specular reflectance effects, we
188 used common preprocessings. Against additive effects, we used data center-
189 ing as recommended by Vandeginste et al. (1998). Against multiplicative
190 effects, we used normalisation as recommended by Martens and Næs (1998).

191 The calibration and test steps were done using Matlab® software (The-
192 MathWorks, Natick, MA, USA) and our own Matlab functions.

193 *2.4. Datasets*

194 In a first step, we have focused our attention on flat leaves in order to
195 study potentiality of our sensor and our correction process. Cut flat leaves
196 measurements were similar to laboratory measurements and we wanted to
197 see if we could obtain similar results as those reported previously. In a
198 second step, architecture effects have been taken into account. We saw in
199 section 2.2 that leaf inclination induced illumination level differences and
200 potential specular reflection. We studied whether it was still possible to
201 calibrate a chemometrical model to predict nitrogen when recorded signal
202 was modified by these phenomena.

203 *2.4.1. Flat leaves*

204 Flag leaves of about 30 various French durum wheat registrated varieties
205 were cut during the 2009 growing season between flowering and maturity.
206 They were dried and conserved in a cold room. Leaves were put on a flat black
207 background (we used the leaf-clip disc of a field spectrometer (FieldSpec®,
208 Analytical Spectral Devices, Inc. (ASD), Boulder, Colorado, USA)). The
209 reference ceramic plate was put beside leaves and the leaves were imaged
210 with the set-up described above. On Figure 3, we can see an image obtained
211 with this protocol.

212 Once images corrected in reflectance (with the process described in para-
213 graph 2.2), regions of interest were drawn on the leaves to calculate a mean
214 reflectance spectrum for each leaf. The corresponding leaf part was send
215 to laboratory for destructive nitrogen concentration measurement (Perkin-
216 Elmer elemental analyser (PE 2400 CHN, CNRS Cefe Montpellier)). No
217 pre-processing was applied on this dataset because leaves were flat-imaged

218 (no specular reflexion, no illumination level issue).

219 *2.4.2. Isolated plants*

220 *Greenhouse plants*

221

222 During winter 2009-2010, several wheat plants were grown in pots in
223 greenhouse with two nitrogen treatments: with or without nitrogen supply.
224 Four French durum wheat registered varieties (Neodur, Primadur, Ixos et
225 Lloyd) were imaged at five phenological stages (tillering, 2 nodes, flowering,
226 450 day-degrees after flowering and maturity). For each plant, the two-upper
227 leaves were marked with coloured plastic collars to be located on the images.
228 After each image (Figure 4), the leaves were cut and send to laboratory for
229 destructive nitrogen measurement. After image correction, regions of interest
230 were drawn on the images to calculate a mean reflectance spectrum for each
231 leaf. In order to take into account illumination level and specular reflexion,
232 two preprocessings were applied on the dataset: normalisation and centering
233 combined in the SNV function.

234

235 *Field plants*

236

237 During the 2010 growing season, wheat field plants were imaged. In
238 order to have isolated plants (to avoid environment effects like multiple re-
239 flections) plants were singled by hand. On each plot, 4 leaves were marked
240 with coloured plastic collars and all the no-marked leaves were cut (see Fig-
241 ure 5). This protocol was repeated 5 times (on the 10th, 20th and 28th of May,
242 the 4th of June and the 1st of July 2010 which correspond to flowering, 165

243 day-degrees after flowering, 260 day-degrees after flowering, 407 day-degrees
244 after flowering and maturity). Once again, the SNV function was used as
245 preprocessing.

246 **3. Results**

247 *3.1. Nitrogen concentration range*

248 On table 1 are summarised the results of laboratory experiments for each
249 dataset.

250 According to the experiments, leaf nitrogen concentration (LNC) varies
251 from 0.4 %DM to 5.88 %DM. Reference LNC values have a quite continuous
252 distribution for the flat leaf dataset and a distribution more segmented (in 2
253 or 3 clusters) for the two other datasets.

254 *3.2. Models calibrated on various datasets*

255 The model on flat leaves (called flat leaf model or M_f in the following)
256 was calibrated without preprocessing. The best model was obtained with 5
257 LV (Figure 6).

258 The optimal processed model on greenhouse plants (called greenhouse
259 model or M_g in the following) required the function SNV (data normalisation
260 and centering)and was calibrated with 6 LV (Figure 7).

261 Data normalisation and centering (SNV function) were also needed to
262 perform the best calibration on field dataset with 4LV (called field model or
263 M_c in the following)(Figure 8).

264 For each of these three models, high R^2 (> 0.8) mean that PLS is rele-
265 vant to extract nitrogen information from reflectance spectra. All the mod-
266 els have a negligible bias, which show the prediction accuracy. Calibration

267 step for each model shows that LNC can be predicted with a rather low
268 SECV (≤ 0.45 %DM). Moreover, the test step (only for flat leaf model and
269 greenhouse leaf model), using new data does not increase so much the error
270 (≤ 0.48 %DM), meaning that there is no overfitting in the model.

271 3.3. Cross-application of models

272 Each model calibrated on isolated plants was applied on the other and
273 vice versa. As the field dataset nitrogen concentration range was only 0-
274 4 %DM, the field model was applied only on the greenhouse dataset whose
275 nitrogen concentration was inside this range (Figure 9).

276 All the data of isolated plants (greenhouse and field plants) were used
277 to calibrate a model. The best model (called isolated plant model or M_t in
278 the following) required once again the function SNV (data normalisation and
279 centering) and called for only 6 LV (Figure 10).

280 Figure 11 shows the PLS-coefficients of model calibrated on isolated
281 plants (greenhouse and field plant datasets together). The coefficient values
282 reveal the importance of each wavelength to build the model. The most im-
283 portant coefficients (in absolute value) correspond to chlorophyll absorption
284 bands (660 nm) but also to other spectral bands: around 500 nm, 550 nm,
285 700 nm, 750 nm and 930 nm.

286 4. Discussion

287 The objective of our work was to evaluate hyperspectral imaging as a non
288 destructive technology to assess leaf nitrogen content in wheat leaves. In this
289 work we used a sensor with a spectral range from 400 to 1000 nm. Our mea-
290 sure leans so mainly on the photosynthetic nitrogen: chlorophyll, chlorophyll

291 a-proteins complexes at 675 nm (Hopkins, 2003) and some proteins accessible
292 via their $N - H$ bound near 900 nm (Curran, 1989). As the sun was used as
293 light source, correction in reflectance was firstly carried out and next models
294 was calibrated based on PLS approach. To illustrate the potential of the
295 method, calibrations were built in two steps: firstly on dried excised leaves
296 to specify the capacity of this technology to assess LNC and secondly on
297 whole plant to take into account different leaf angles and variable leaf water
298 content in the model. On excised dried flat leaves, a good accurate model was
299 performed (Figure 6). Statistical parameters of this prediction were pretty
300 good: the R^2 - which measures the accuracy of regression - was closed to 1
301 (0.903), the prediction error did not exceed 16% of the mean of the dataset,
302 and bias was negligible. These results are similar to those obtained by Morón
303 et al. (2007) ($R^2=0.88$ and $SECV=0.27$). Obviously they demonstrate the
304 relevance of our sensor and validate our reflectance correction process to infer
305 leaf nitrogen concentration with a good relevance.

306

307 In a second step, LNC was inferred from leaf spectra collected on fresh and
308 non excised leaves from greenhouse or field plants. In both cases, calibrations
309 obtained have a good accuracy: R^2 values remain high (> 0.889), prediction
310 errors do not exceed 15% of the mean of the dataset and, as previously, the
311 bias was negligible (Figures 7 and 8). These results are slight higher than
312 those obtained previously by Morón et al. (2007) ($R^2=0.82$ and $SECV=0.74$
313 in laboratory with a spectrometer equipped with an internal light). The
314 combination of reflectance correction process and pre-processings (data nor-
315 malisation and centering) was very efficient to take into account different

316 leaf inclinations on plants and possible specular reflection: our calibration
317 quality decreases slightly but remains very relevant. These results suggest
318 strongly that it possible to assess leaf nitrogen concentration directly from
319 fresh leaves during plant cycle following a non destructive approach.

320

321 Although all these different models provide accurate leaf nitrogen predic-
322 tion, these models were built on different bases. Therefore, a model built
323 on a given dataset was not relevant to the next one: for example calibration
324 on fresh field leaves could not be used on greenhouse leaves: the prediction
325 bias is too high (Figure 9(a)) indicating that in our case models are dataset
326 dependent. Both low sample number and growing conditions (especially
327 plant nitrogen supply) could explain these differences. Correlations between
328 leaf characteristics (physical properties as thickness, biochemical composi-
329 tion such as chlorophyll, protein content, etc.) and LNC may vary from one
330 experiment to the other and affect the relative importance of the different
331 wavelengths involved in the PLS process. Otherwise, as we underlined it in
332 introduction, the relation between photosynthetic nitrogen and total nitro-
333 gen could vary according to environmental conditions, leaf age, etc. Anyway,
334 pooling the two datasets (plants in greenhouse and in field) let us to propose
335 a common model (Figure 10). The high R^2 (0.875), the low SEPc and the
336 negligible bias mean that variable growing conditions of the samples do not
337 prevent from accessing to nitrogen information. The model coefficients of
338 the plant model Mt (Figure 11) show that many spectral bands are solicited
339 and not only chlorophyll absorption bands. We can thus think that using
340 the whole spectra allow us to include chlorophyll-nitrogen relation variability

341 inside the PLS model. Indeed, Hansen and Schjoerring (2003) showed that
342 using PLS improved the prediction (by 24 %) of the nitrogen concentration
343 with regard to the use of vegetation indices as the NDVI for example. The
344 results obtained by combining all the datasets suggest that including a larger
345 dataset would allow to obtain a satisfactory robustness, provided every possi-
346 ble situation is represented in the samples. For that it is necessary to include
347 several genotypes, several growing years and different growing conditions (in
348 greenhouse and in field) and particularly plant density.

349 **5. Conclusion**

350 A few main conclusions can be established from this study. First, nitrogen
351 concentration is accessible from reflectance spectra in 400-1000 nm range not
352 only from dried leaves but also from fresh samples scanned on whole plants.
353 Secondly, reflectance correction process and pre-processings used allow to free
354 oneself from solar lighting issues and plant architecture effects (illumination
355 level and specular reflection) leading to the same quality than the models
356 obtained with laboratory spectra. Moreover, using the whole spectra allow
357 us to overcome variability due to growing conditions, compared to the use
358 of only chlorophyll absorption bands. Nevertheless, a wide calibration set is
359 necessary to calibrate models robust to growing conditions, year, etc.

360
361 Finally, this study showed that field close range hyperspectral imaging is
362 a promising technology for non destructive nitrogen monitoring. Its use can
363 be enlarged to physiology or modeling issues. Applying this chemometrical
364 model on whole plot hyperspectral images produces spatial nitrogen cartogra-

365 phies. It will be thus possible to follow-up nitrogen dynamics at each leaf
366 level. Data can be introduced in growing models or nitrogen remobilisation
367 models for example.

368 **Acknowledgements**

369 This study has been funded by the Garicc project of the Q@liméditerranée
370 competitive cluster. We are very grateful to Frédéric Compan and Béatrice
371 Ramora for their help for field experiments.

372 **References**

- 373 Alchanatis, V., Schmilovitch, Z., 2005. In-field assessment of single leaf ni-
374 trogen status by spectral reflectance measurements. *Precision Agriculture*
375 6, 25–39.
- 376 Baret, F., Fourty, T., 1997. Diagnosis on the Nitrogen Status in Crops. G.
377 Lemaire (ed), Ch. Radiometric Estimates of Nitrogen Status of Leaves and
378 Canopies, pp. 201–227.
- 379 Bélanger, G., Walsh, J., Richards, J., Milburn, P., Ziadi, N., 2001. Critical
380 nitrogen curve and nitrogen nutrition index for potato in eastern canada.
381 *American Journal of Potato Research* 78 (5), 355–364.
- 382 Bousquet, L., Lachérade, S., Jacquemoud, S., Moya, I., 2005. Leaf brdf mea-
383 surements and model for specular and diffuse components differentiation.
384 *Remote Sensing of Environment* 98 (2-3), 201–211.

- 385 Chelle, M., 2006. Could plant leaves be treated as lambertian surfaces in
386 dense crop canopies to estimate light absorption? *Ecological Modelling*
387 198 (1-2), 219–228.
- 388 Chen, P., Haboudane, D., Tremblay, N., Wang, J., Vigneault, P., Li, B., 2010.
389 New spectral indicator assessing the efficiency of crop nitrogen treatment
390 in corn and wheat. *Remote Sensing of Environment* 114 (9), 1987–1997.
- 391 Colnenne, C., Meynard, J., Reau, R., Justes, E., Merrien, A., 1998. Determi-
392 nation of a critical nitrogen dilution curve for winter oilseed rape. *Annals*
393 *of Botany* 81 (2), 311–317.
- 394 Curran, P. J., 1989. Remote sensing of foliar chemistry. *Remote Sensing of*
395 *Environment* 30, 271–278.
- 396 Evans, J., 1983. Nitrogen and photosynthesis in the flag leaf of wheat
397 (*Triticum aestivum* L.). *Plant Physiology* 72, 297–302.
- 398 Farrugia, A., Gastal, F., Scholefield, D., 2004. Assessment of nitrogen status
399 of grassland. *Grass Forage Sci.* 59 (2004), 113-120.
- 400 Fitzgerald, G., Rodriguez, D., O’Leary, G., 2010. Measuring and predict-
401 ing canopy nitrogen nutrition in wheat using a spectral index-the canopy
402 chlorophyll content index (ccci). *Field Crops Research* 116 (3), 318–324.
- 403 Fox, R., Piekielek, W., Macneal, K., 2001. Comparison of late-season di-
404 agnostic tests for predicting nitrogen status of corn. *Agronomy Journal*
405 93 (3), 590–597.

- 406 Grant, L., 1987. Diffuse and specular characteristics of leaf reflectance. *Re-*
407 *mote Sensing of Environment* 22 (2), 309–322.
- 408 Hansen, P., Schjoerring, J., 2003. Reflectance measurement of canopy
409 biomass and nitrogen status in wheat crops using normalized difference
410 vegetation indices and partial least square regression. *Remote Sensing of*
411 *Environment* 86, 542–553.
- 412 Hidema, J., Makino, A., Mae, T., Ojima, K., 1991. Photosynthetic charac-
413 teristics of rice leaves aged under different irradiances from full expansion
414 through senescence. *Plant Physiology* 97, 1287–1293.
- 415 Hopkins, W. G., 2003. *Physiologie végétale*. Bruxelles : De Boeck.
- 416 Houllès, V., Guérif, M., Mary, B., 2007. Elaboration of a nitrogen nutrition
417 indicator for winter wheat based on leaf area index and chlorophyll content
418 for making nitrogen recommendations. *European Journal of Agronomy*
419 27 (1), 1–11.
- 420 Justes, E., Mary, B., Meynard, J., Machet, J., Thelier-Huche, L., 1994. De-
421 termination of a critical nitrogen dilution curve for winter wheat crops.
422 *Annals of Botany* 74 (4), 397–407.
- 423 Kokaly, R., 2001. Investigating a physical basis for spectroscopic estimates of
424 leaf nitrogen concentration. *Remote Sensing of Environment* 75 (2), 153–
425 161.
- 426 Lee, W., Searcy, S., Kataoka, T., 1999. Assessing nitrogen stress in corn
427 varieties of varying color. In: 1999 ASAE Annual International Meeting.

- 428 No. Paper No 99-3034 in ASAE Meeting Presentation. ASAE, 2950 Niles
429 Rd., St. Joseph, MI 49085-9659 USA, Toronto, Ontario Canada.
- 430 Lemaire, G., Gastal, F., 1997. Diagnosis of the Nitrogen Status in Crops.
431 G. Lemaire (Ed.), Ch. N Uptake and Distribution in Plant Canopies, pp.
432 3–43.
- 433 Lemaire, G., Jeuffroy, M.-H., Gastal, F., 2008. Diagnosis tool for plant and
434 crop N status in vegetative stage. theory and practices for crop N manage-
435 ment. *European Journal of Agronomy* 28 (4), 614–624.
- 436 Lemaire, G., Salette, J., 1984. Relationship between dynamics of growth and
437 of nitrogen uptake in a pure grass stand. i. study of environmental effects.
438 *Agronomie* 4, 423–430.
- 439 Martens, H., Næs, T., 1998. *Multivariate calibration*. John Wiley & Sons.
- 440 Morón, A., García, A., Sawchik, J., Cozzolino, D., 2007. Preliminary study on
441 the use of near-infrared reflectance spectroscopy to assess nitrogen content
442 of undried wheat plants. *Journal of the Science of Food and Agriculture*
443 87 (1), 147–152.
- 444 Sheehy, J., Dionora, M., Mitchell, P., Peng, S., Cassman, K., Lemaire, G.,
445 Williams, R., 1998. Critical nitrogen concentrations: Implications for high-
446 yielding rice (*Oryza sativa* L.) cultivars in the tropics. *Field Crops Research*
447 59 (1), 31–41.
- 448 Spaner, D., Todd, A., Navabi, A., McKenzie, D., Goonewardene, L., 2005.
449 Can leaf chlorophyll measures at differing growth stages be used as an in-

- 450 indicator of winter wheat and spring barley nitrogen requirements in eastern
451 canada? *Journal of Agronomy and Crop Science* 191 (5), 393–399.
- 452 Vandeginste, B. G. M., Massart, D. L., Buydens, L. M. C., De Jong, S., Lewi,
453 P. J., Smeyers-Verbeke, J., 1998. *Handbook of Chemometrics and Quali-*
454 *metrics: Part B. Vol. 20B of Data Handling in Science and Technology.*
455 Elsevier Science.
- 456 Wold, S., Sjöström, M., Eriksson, L., 2001. *Pls-regression: a basic tool of*
457 *chemometrics. Chemometrics and Intelligent Laboratory Systems* 58, 109–
458 130.
- 459 Ziadi, N., Bélanger, G., Claessens, A., Lefebvre, L., Cambouris, A., Tremblay,
460 N., Nolin, M., Parent, L.-E., 2010. Determination of a critical nitrogen
461 dilution curve for spring wheat. *Agronomy Journal* 102 (1), 241–250.
- 462 Ziadi, N., Brassard, M., Bélanger, G., Claessens, A., Tremblay, N., Cam-
463 bouris, A., Nolin, M., Parent, L.-E., 2008. Chlorophyll measurements and
464 nitrogen nutrition index for the evaluation of corn nitrogen status. *Agron-*
465 *omy Journal* 100 (5), 1264–1273.

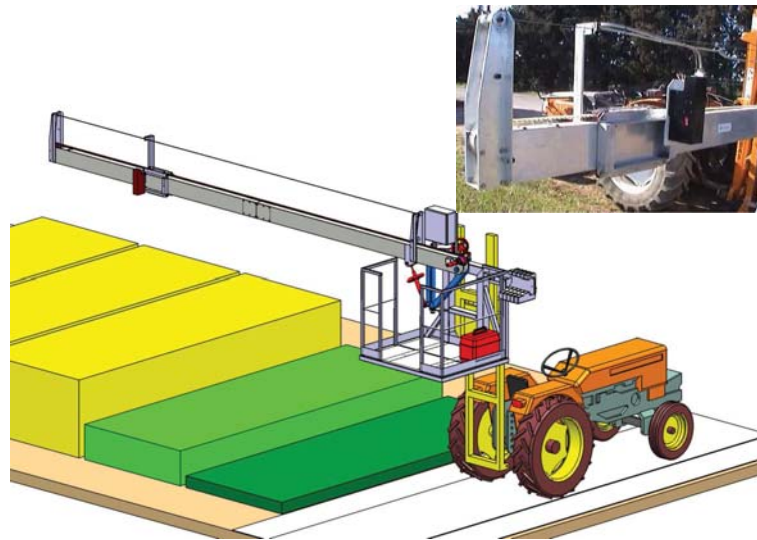
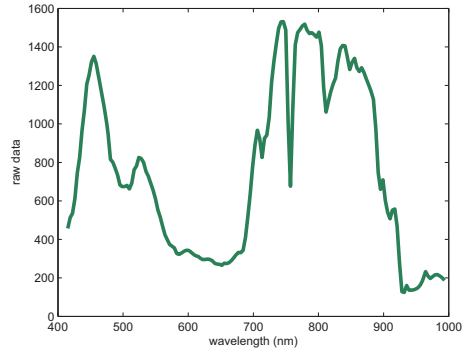


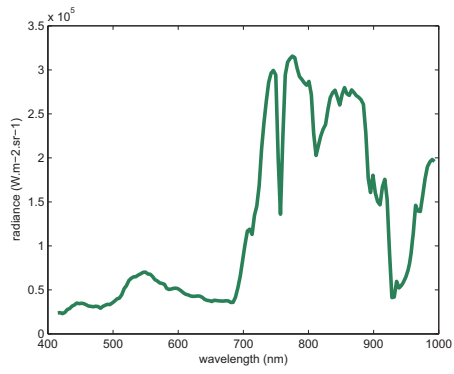
Figure 1: Hyperspectral imaging set-up.

Table 1: Nitrogen concentration range for each dataset: nitrogen concentrations are in %DM

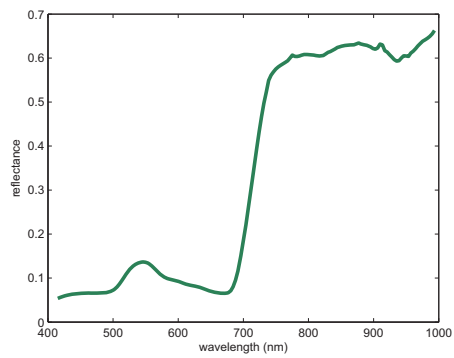
dataset	n	min	max	mean	standard deviation
flat leaves	146	0.4	3.78	2.07	1.05
greenhouse plants	180	0.81	5.88	3.22	1.42
field isolated plants	56	0.71	4.2	2.37	1.07



(a)



(b)



(c)

Figure 2: Example of (a) raw, (b) radiance and (c) reflectance spectra for an isolated leaf. Absorption peaks due to the atmosphere are removed in (c) by the reflectance correction.

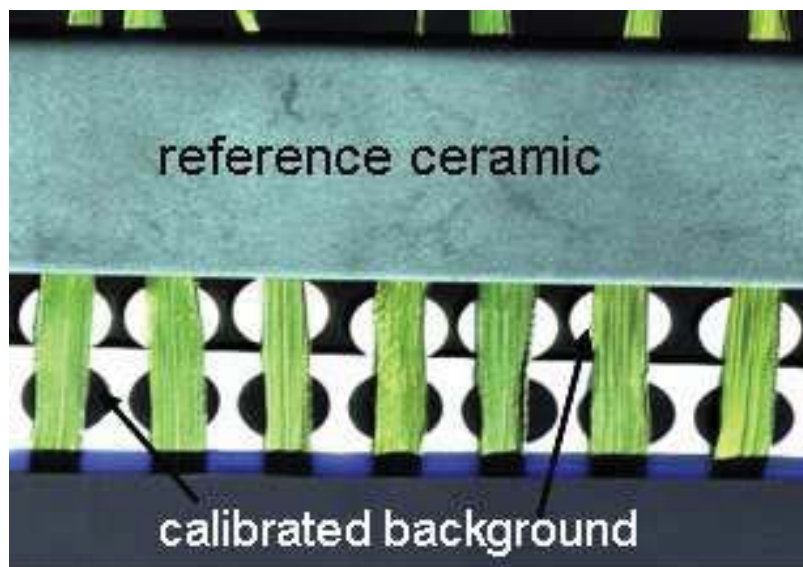
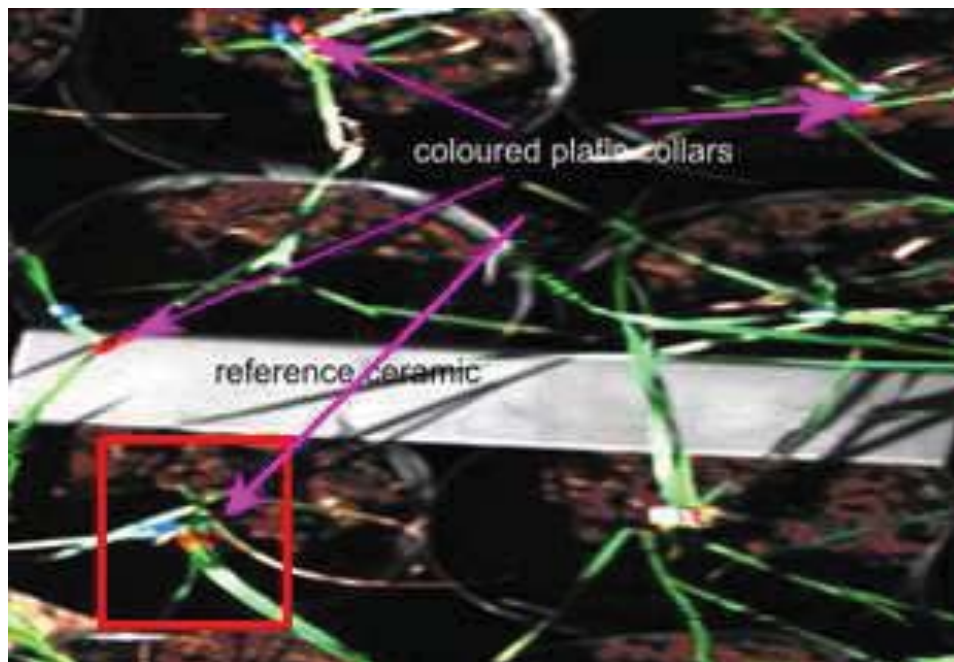
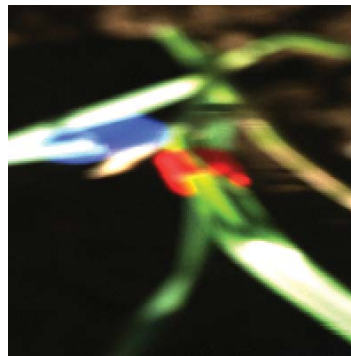


Figure 3: Example of an image obtained with the protocol for flat leaves (black and white background discs were set but only black ones are used in this study).



(a)



(b)

Figure 4: Example of an image obtained with the protocol for greenhouse plants.

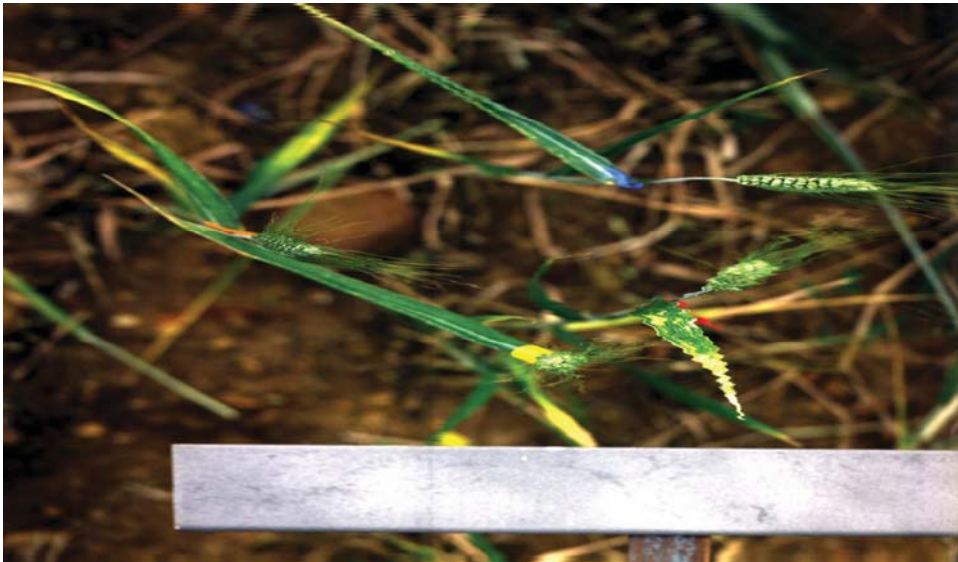


Figure 5: Example of an image obtained with the protocol for field isolated plants.

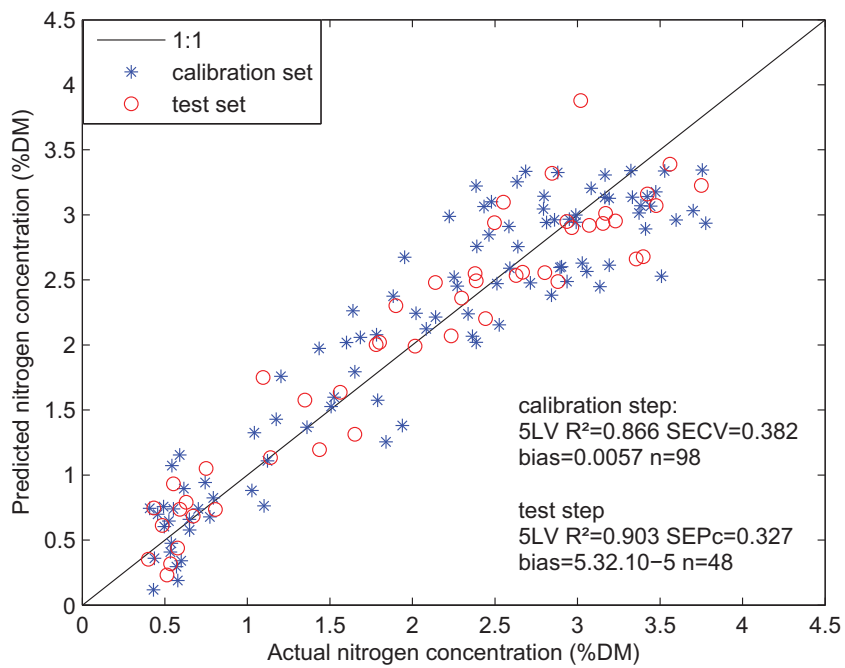


Figure 6: Results of the chemometrical model calibrated on flat leaves with no preprocessing and 5LV (blue stars for calibration step and red circles for test step).

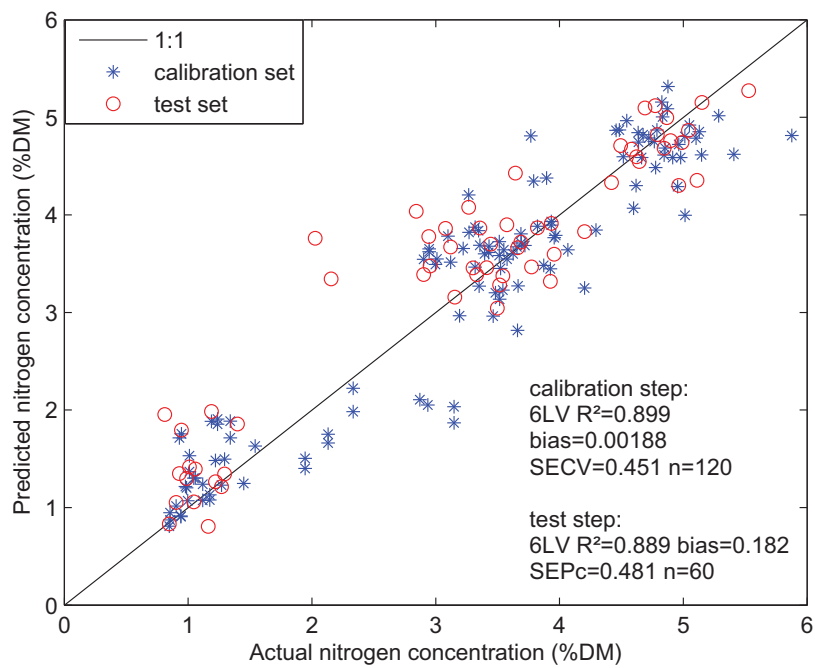


Figure 7: Results of the chemometrical model calibrated on greenhouse plants with SNV and 6LV (blue stars for calibration step and red circles for test step).

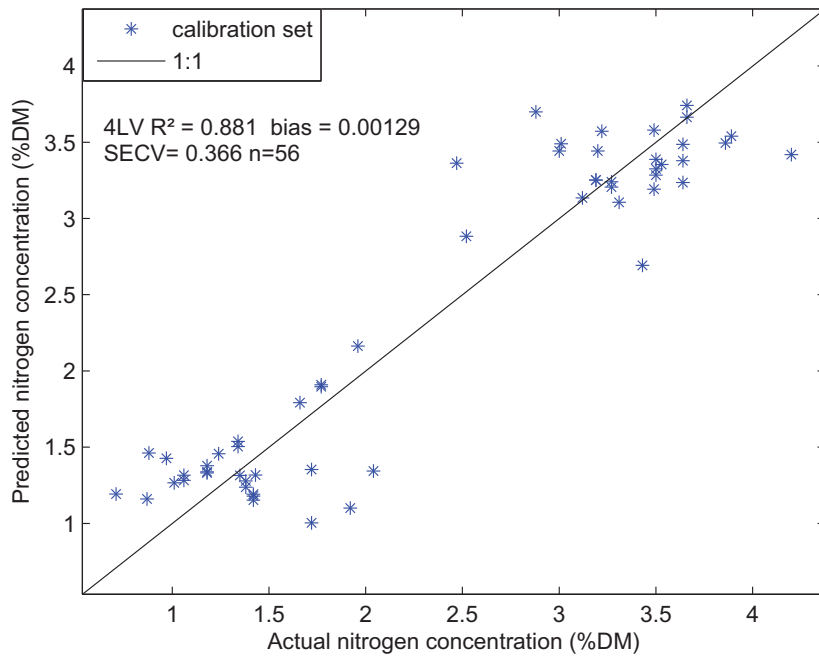
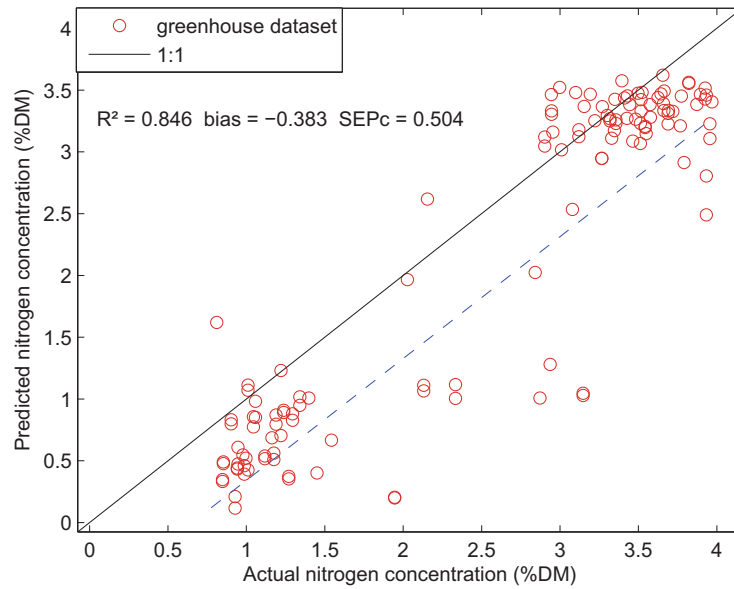
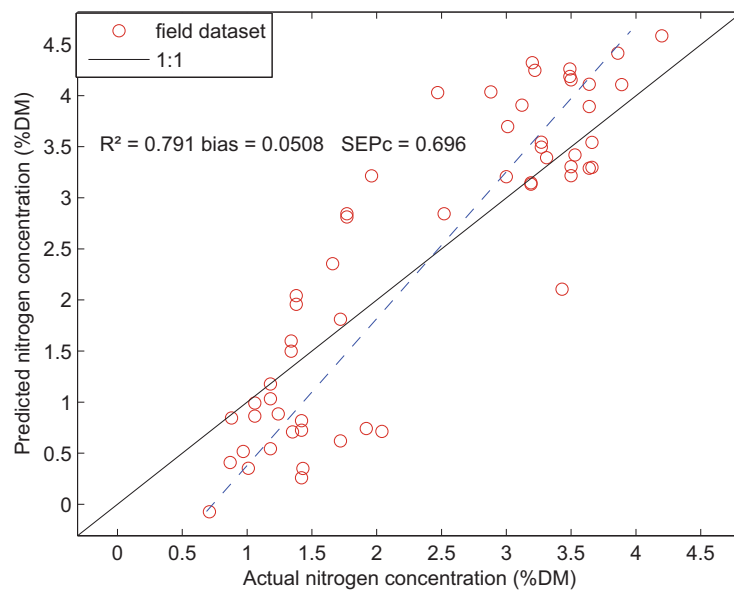


Figure 8: Results of the chemometrical model calibrated on field isolated plants with SNV and 4LV.



(a)



(b)

Figure 9: Cross-application of the models calibrated on isolated plants: (a) model calibrated on field plants applied on greenhouse plants, (b) model calibrated on greenhouse plants applied on field plants.

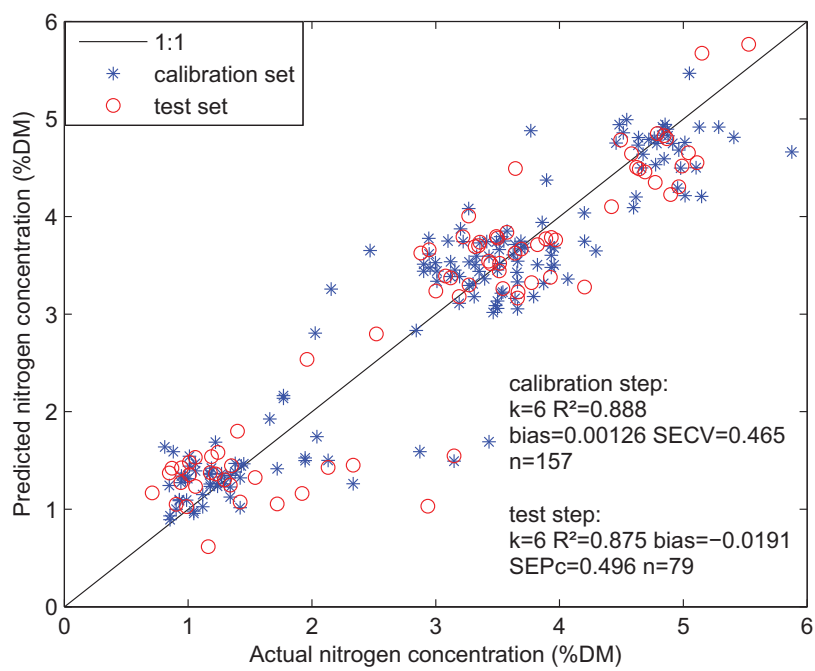


Figure 10: Results of the chemometrical model calibrated on isolated plants (greenhouse and field plants) with SNV and 6LV (blue stars for calibration step and red circles for test step).

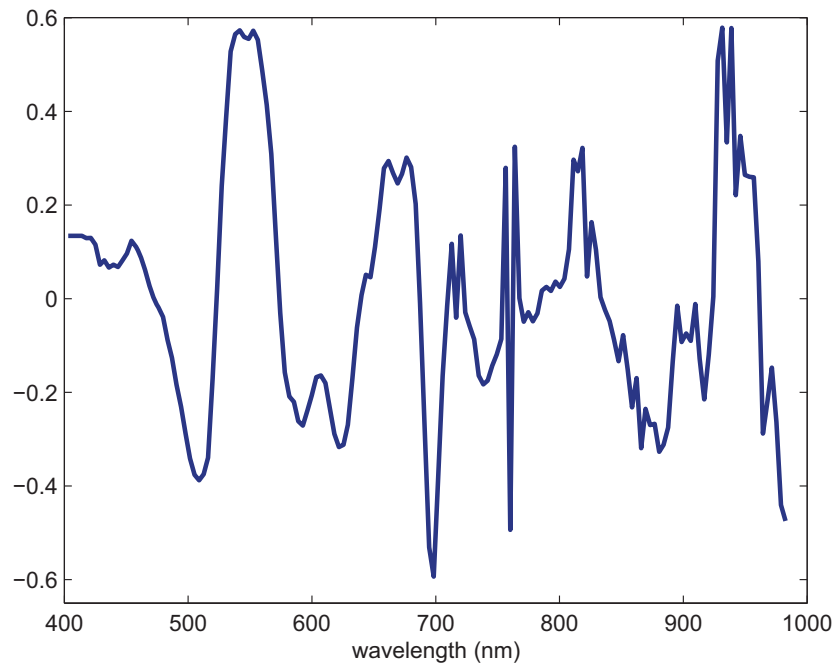


Figure 11: PLS-coefficients for the isolated plant models M_t .